



## Research

## AI for Process Manufacturing—Article

# Toward Intelligent and Green Ethylene Manufacturing: An AI-Based Multi-Objective Dynamic Optimization Framework for the Steam Thermal Cracking Process



Yao Zhang<sup>a</sup>, Peng Sha<sup>b</sup>, Meihong Wang<sup>a,\*</sup>, Cheng Zheng<sup>b</sup>, Shengyuan Huang<sup>a</sup>, Xiao Wu<sup>b,\*</sup>, Joan Cordiner<sup>a</sup>

<sup>a</sup>School of Chemical, Materials and Biological Engineering, The University of Sheffield, Sheffield S1 3JD, UK

<sup>b</sup>National Engineering Research Center of Power Generation Control and Safety, School of Energy and Environment, Southeast University, Nanjing 210096, China

## ARTICLE INFO

## Article history:

Received 5 November 2024

Revised 11 March 2025

Accepted 11 June 2025

Available online 5 August 2025

## Keywords:

Green manufacturing

Thermal cracking furnace

Artificial intelligence

Hybrid modeling

Multi-objective optimization

Process modeling

## ABSTRACT

With growing concerns over environmental issues, ethylene manufacturing is shifting from a sole focus on economic benefits to an additional consideration of environmental impacts. The operation of the thermal cracking furnace in ethylene manufacturing determines not only the profitability of an ethylene plant but also the carbon emissions it releases. While multi-objective optimization of the thermal cracking furnace to balance profit with environmental impact is an effective solution to achieve green ethylene manufacturing, it carries a high computational demand due to the complex dynamic processes involved. In this work, artificial intelligence (AI) is applied to develop a novel hybrid model based on physically consistent machine learning (PCML). This hybrid model not only reduces the computational demand but also retains the interpretability and scalability of the model. With this hybrid model, the computational demand of the multi-objective dynamic optimization is reduced to 77 s. The optimization results show that dynamically adjusting the operating variables with coke formation can effectively improve profit and reduce CO<sub>2</sub> emissions. In addition, the results from this study indicate that sacrificing 28.97% of the annual profit can significantly reduce the annual CO<sub>2</sub> emissions by 42.89%. The key findings of this study highlight the great potential for green ethylene manufacturing based on AI through modeling and optimization approaches. This study will be important for industrial practitioners and policy-makers.

© 2025 THE AUTHORS. Published by Elsevier LTD on behalf of Chinese Academy of Engineering and Higher Education Press Limited Company. This is an open access article under the CC BY license (<http://creativecommons.org/licenses/by/4.0/>).

## 1. Introduction

### 1.1. Background

Ethylene is one of the most important building blocks in the petrochemical industry, and demand for it is increasing [1,2]. The thermal cracking furnace is the core equipment in ethylene manufacturing, as it not only directly determines the yields of final products but is also one of the most energy-intensive pieces of equipment [3]. The high energy consumption of a thermal cracking furnace is due to the high temperatures required for cracking reactions to take place (typically 1073–1373 K for different feedstocks). Burners located at the bottom of the thermal cracking furnace generate a large amount of heat by burning fossil fuels, leading to sig-

nificant carbon dioxide (CO<sub>2</sub>) emissions [4]. In 2023, the thermal cracking process for ethylene production worldwide resulted in over 260 million metric tons of CO<sub>2</sub> emissions [5]. Therefore, in the context of global warming, ethylene manufacturing has shifted from a sole focus on maximizing profit toward an emphasis on green production that simultaneously considers economic benefits and environmental impact.

In process manufacturing, such as ethylene manufacturing, modeling-based process analysis, design, and optimization are commonly used to increase economic benefits [2]. However, the simultaneous heat transfer, chemical reactions, and coke formation in ethylene manufacturing, along with their interactions, make such methods of increasing profit challenging—especially regarding the decision variables, which must be adjusted with coke formation at every time interval in a dynamic optimization. On the other hand, considering the environmental impact of thermal cracking furnaces, various technologies including combined carbon capture and storage (CCS), oxy-fuel combustion, and the use of

\* Corresponding authors.

E-mail addresses: [Meihong.Wang@sheffield.ac.uk](mailto:Meihong.Wang@sheffield.ac.uk) (M. Wang), [wux@seu.edu.cn](mailto:wux@seu.edu.cn) (X. Wu).

electric cracking furnaces have been proposed and studied to reduce CO<sub>2</sub> emissions [4,6,7]. However, the high capital costs, technical complexities, and need for additional infrastructure associated with these new technologies have constrained their widespread adoption. Integrating post-combustion carbon capture technology with the steam cracking process presents significant economic challenges, with capital costs reaching up 26.041 million USD and additional operational costs of 6.24 million USD [4]. Similarly, the significant economic costs and energy consumption associated with pure oxygen production present unavoidable obstacles to the application of oxy-fuel combustion in the steam cracking process. Furthermore, implementing oxy-fuel combustion in existing thermal cracking furnaces would lead to flame instability, requiring extensive equipment modifications [8]. While electric cracking furnaces have attracted increasing attention in recent studies, their large-scale industrial application remains limited due to two primary factors: Firstly, the design and construction of new-generation electric cracking furnaces would fundamentally differ from traditional thermal cracking furnaces; and secondly, the relatively high cost of electricity compared with natural gas presents a significant economic barrier to the implementation of electric furnaces [7]. Thus, multi-objective optimization considering both the profit and CO<sub>2</sub> emissions from existing thermal cracking furnaces is an effective approach for achieving green ethylene manufacturing. However, the challenges of dynamic optimization remain, especially when multiple objectives are considered. Thanks to rapid advances in computer science, artificial intelligence (AI) can provide promising solutions to the challenges described above through hybrid modeling (HM). Combining machine learning with first-principles modeling (FPM) can increase model accuracy and reduce computational demand while retaining the interpretability and scalability of FPM. With the strengths of both approaches, HM can provide robust and efficient solutions for the optimization of thermal cracking furnaces. Therefore, the use of AI to assist in achieving green ethylene manufacturing is very promising.

## 1.2. Literature review

As the thermal cracking furnace is the core equipment in ethylene manufacturing, many studies have aimed to improve its production efficiency and economic benefits through modeling, simulations, process analyses, and optimization. Masoumi et al. [9] established a dynamic model of the plug flow reactor (PFR) in a thermal cracking furnace considering coke formation. Using this model, the temperature profile was optimized to achieve maximum operating profit. Their study offers valuable insights into the optimal operating temperature range for the PFR in an ethylene cracking furnace. However, the optimization was steady-state, meaning that the temperature profile was not adjusted in response to changes in the coke layer at different time intervals. More importantly, another crucial operational parameter, the feedstock-to-diluent ratio, was not considered as a decision variable in this optimization. Gao et al. [10] performed steady-state modeling and simulation of the PFR using Aspen HYSYS<sup>®</sup>, analyzing the impact of the coil outlet temperature (COT) and feedstock-to-diluent ratio on the yields of valuable products. Subsequently, an optimization was carried out with the COT and feedstock-to-diluent ratio as the decision variables and with economic profitability as the objective function. This steady-state optimization accounted for the economic penalties of decoking, providing guidance on the trade-off between valuable product yields and the run length of the PFR. However, since a steady-state model was used, the optimization study used the coking rate under clean tube conditions for the entire run length, failing to account for the dynamic impact of coking on the process. Building on the research by Gao

et al. [10], Berreni and Wang [11] developed a dynamic model and conducted both steady-state and dynamic optimizations. The operating variables were adjusted over time to account for the dynamic impact of coking, resulting in higher profit. The results indicated that annual profits could be increased by 13.1% under dynamic optimization compared with steady-state optimization. However, dynamic optimization based on FPM has a very high computational demand, with the optimization in that study taking 19 h to complete.

Given increasing concerns regarding climate change and the signing of the Paris Agreement, the focus of research on thermal cracking furnaces has shifted from solely addressing economic benefits to balancing the trade-off between profit and environmental impact. Yu et al. [12] developed a data-driven model for thermal cracking furnaces and used this model to optimize two important and conflicting objectives: maximizing the yields of key products and minimizing the fuel consumption per unit of ethylene produced. Their study provides valuable guidance for improving the energy efficiency of the thermal cracking furnace. Shen et al. [13] developed a data-driven model for the thermal cracking furnace and a life-cycle assessment model to determine its environmental impacts. Based on these two models, they conducted a multi-objective optimization that considered both environmental impact and economic benefits. The findings of their study offer significant insights into reducing CO<sub>2</sub> emissions while ensuring reasonable profits. However, both studies only carried out steady-state optimizations, which fail to consider the dynamic impact of coking during the cracking process [12,13]. As a result, the influence of decision variables on the run length of a thermal cracking furnace, as well as the economic penalties and environmental impacts associated with decoking, have not been adequately addressed.

It can be observed that, whether the studies described above focus solely on economic benefits or consider both profits and environmental impact, few carry out dynamic optimization, adjusting decision variables in response to coke formation at every time interval. This is because dynamic optimization has a significantly higher computational demand than steady-state optimization. However, several existing studies have shown that the use of AI can reduce model complexities in chemical engineering through HM [14]. For example, Rezaei et al. [15] developed a hybrid model to reduce the computational demand of the FPM of a multi-PFR system for methanol synthesis through an extended Kalman filter. The resulting hybrid model with reduced computational demand was found to be suitable for online monitoring and control applications. Bui et al. [16] used an empirical partial least-squares model to reduce the model complexities of heterogeneously catalyzed reactors. Their integrated hybrid model could be used for monitoring and predicting catalyst lifetime in operational industrial processes. These two studies [15,16] successfully reduced the computational demand of FPM for online applications while retaining the interpretability of the model through a data-driven modeling (DM) approach. However, this HM approach cannot ensure the scalability of the model. Xiao and You [17,18] proposed a physically consistent deep learning (PCDL)-based modeling approach to improve building energy efficiency and indoor thermal comfort by adding the physical information contained in FPM to DM training in the form of physics consistency. The results of these studies showed that this novel approach makes it possible to train DM with less data and has high accuracy in the data range out of the training data. In contrast to the monotonous physics consistency of the thermal model of building, the thermal cracking process exhibits physics consistency with higher complexity. Embedding the physics consistency of the thermal cracking process in the construction of a novel hybrid model will allow the model to retain interpretability and scalability while reducing the

computational demand, making it suitable for multi-objective dynamic optimization.

### 1.3. Aim and novel contributions

This paper aims to carry out a multi-objective dynamic optimization to maximize the profit and minimize the CO<sub>2</sub> emissions for a thermal cracking furnace, considering the entire operational cycle (i.e., production time and decoking time), based on a physically consistent machine learning (PCML) hybrid model. In comparison with previous studies, this study makes the following novel contributions:

(1) **A multi-objective optimization is carried out that considers both the economic benefits and the environmental impacts of a thermal cracking furnace.** Thus far, few studies have examined the trade-off between the economic benefits and environmental impact of a thermal cracking furnace. Although the studies by Yu et al. [12] and Shen et al. [13] suggested the modification of different operating variables under clean tube conditions to make ethylene production green, they did not discuss how these operating variables should be adjusted with coke formation at different time intervals. Berreni and Wang [11] recommended increasing the COT with coke formation to ensure conversion of the feedstock—an adjustment that would contribute to increasing the profit. However, increasing the COT with coke formation would lead to higher energy consumption and CO<sub>2</sub> emissions, and the environmental impact of these adjustments are not addressed in their study. In this study, we carry out a multi-objective dynamic optimization based on a PCML hybrid model to guide operation for the whole production time.

(2) **A PCML-based hybrid model for the multi-objective dynamic optimization of a thermal cracking furnace is developed, which can reduce the computational demand while retaining the interpretability and scalability of FPM.** Because of the occurrence of coking, the optimization of the operating variables for a thermal cracking furnace should be dynamic, since the operating variables should be optimally adjusted according to the different thicknesses of the coke layer. This hybrid model reduces the computational demand of the FPM through machine learning and maintains the interpretability and scalability of the model by embedding the physical information contained in the FPM in the form of physics consistency into the machine learning training. The optimization results of this newly developed PCML-based hybrid model are more reliable in the operating range, with low data requirements for machine learning. Moreover, compared with existing HM methods [15,16], our PCML-based hybrid model demonstrates broader applicability, particularly in addressing complex nonlinear systems. Existing HM methods typically combine FPM with DM, such as partial least squares [16] or Kalman filters [15], which often rely on linear assumptions between inputs and outputs, thereby failing to effectively address nonlinear relationships. In addition, the proposed PCML-based hybrid model incorporates stronger physical interpretability. Although existing HM methods can retain partial physical information by generating data through FPM for training [15,16], such information tends to lack clarity and specificity. The proposed hybrid model explicitly extracts and embeds physical information in the form of physics consistency into the training of DM, significantly increasing the interpretability of the hybrid model. Furthermore, the embedding of physics consistency into the PCML-based hybrid model is relatively straightforward to implement, compared with the complex structures of other hybrid models. This feature makes it possible for engineers with extensive process experience but limited machine learning expertise to develop and use this kind of HM approach. However, the proposed approach is strongly dependent on the accuracy of the FPM used. Thus, when different types of

feedstock are used for steam thermal cracking, a new FPM must be developed and validated. In addition, as the reaction mechanisms vary across feedstock types, the extracted physics consistency also differs.

(3) **The environmental impact of the decoking process is considered for the first time when performing a multi-objective optimization for a thermal cracking furnace.** Although the expense and product penalties of the decoking process have been previously considered, the environmental impact of the decoking process has not been carefully studied. Frequent shutdowns can result in large amounts of CO<sub>2</sub> emissions. By predicting the PFR run length, the energy consumption during the decoking process, and the coking layer distribution at shutdown, this study investigates the impact of the operating variables on the trade-offs between economic benefits and environmental impact throughout the operational cycle.

## 2. PCML-based hybrid modeling

### 2.1. Process description

As shown in Fig. 1, a typical PFR operational cycle in a thermal cracking furnace starts under clean tube conditions (stage 1). At this stage, the preheated feedstock and diluent enter the radiation section of the thermal cracking furnace, where the thermal cracking reactions take place at temperatures between 1073 and 1373 K. This process decomposes the feedstock into ethylene and propylene (i.e., valuable products) and other byproducts; it also causes coke formation on the inner tube wall of the PFR (stage 2). Burners in the radiation section combust liquid natural gas (LNG) to maintain the high temperatures required for the cracking reactions in the PFR, generating significant amounts of CO<sub>2</sub> emissions [19]. Compared with clean tube conditions, a PFR with a coke layer on the inner tube wall has a lower heat transfer efficiency, smaller reaction volume, and higher pressure drop [20]. To sustain the conversion rate of the feedstock and ensure economic benefits, the PFR requires a higher temperature profile, which leads to increased CO<sub>2</sub> emissions and faster coking rates. As a result, it is important to carefully adjust the operating variables with coke formation in order to weigh the economic benefits against the environmental impacts.

This study explores the economic loss and environmental impact of the decoking process. The thermal cracking furnace must

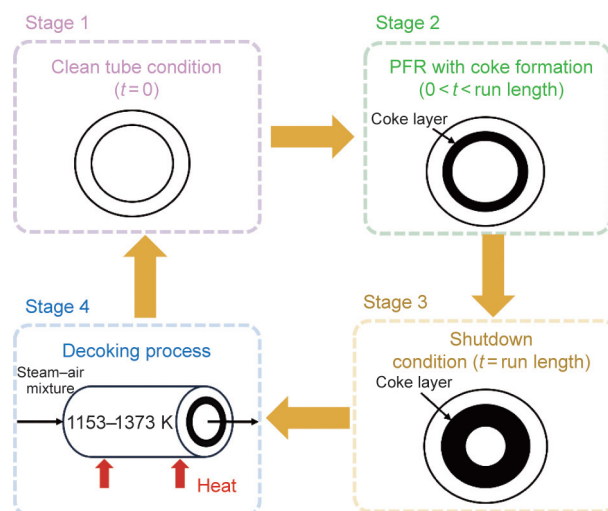


Fig. 1. A typical PFR operational cycle in a thermal cracking furnace.  $t$ : production time.

be shutdown for 24–48 h for decoking once the coke layer on the PFR's inner surface reaches a certain limit (stage 3) [21]. During the decoking process (stage 4), a high-pressure steam–air mixture is fed into the furnace and heated to 1153–1373 K to react with the coke on the inner tube wall of the PFR [22]. Frequent decoking results in production downtime, increased maintenance and energy costs, and accelerated equipment wear, thereby negatively impacting the economic efficiency of the furnace. Environmentally, the frequent need for decoking contributes to increased CO<sub>2</sub> emissions, as well as higher energy and water consumption. Among various environmental concerns, reducing CO<sub>2</sub> emissions is particularly significant for achieving green ethylene manufacturing. During the decoking process, a substantial amount of CO<sub>2</sub> is generated both indirectly through energy consumption and directly through the reaction of the coke layer on the PFR's inner wall with the steam–air mixture. Thus, the economic loss and environmental impact associated with decoking are significant and cannot be overlooked. To consider the entire operational cycle, the effects on the decoking frequency of adjusting the operating variables with varying coke thickness should be carefully evaluated, in addition to the trade-off between the economic benefits and the environmental impact during the run length.

## 2.2. Hybrid modeling

### 2.2.1. FPM and physics consistency

A pseudo-dynamic model considering the interactions among heat transfer, chemical reactions, and coke formation was developed in our previous work and validated with industrial data [23,24]. This model was implemented in gPROMS ModelBuilder® using the configuration of a pilot scale PFR (Table 1) [25] to generate data.

Physics consistency is extracted from the material balance, reaction rate, coking rate, and coke thickness equations, which are shown below [24]:

$$\frac{\partial F_i(z)}{\partial z} = \sum_{j=1}^{NR} S_{ij} \times r_j(z) \times M_{wi} \times \frac{\pi \times D(z)^2}{4} \quad (1)$$

where  $z$  is the distribution domain along the axial direction of PFR,  $F_i$  is the mass flow rate of component  $i$ , NR is the number of reactions,  $S_{ij}$  is the stoichiometry coefficient,  $M_{wi}$  is the molecular weight of component  $i$ ,  $D$  is the inner diameter of PFR with coke formation, and  $r_j$  is the reaction rate of reaction  $j$ , which can be calculated as follows:

$$r_j(z) = A_j \times e^{\frac{-E_{aj}}{RT(z)}} \times \prod_{i=1}^{NC} C_i^{n_{ij}}(z) \quad (2)$$

where  $A_j$  is the pre-exponential factor for reaction  $j$ ,  $E_{aj}$  is the activation energy of reaction  $j$ ,  $R$  is the universal gas constant,  $T$  is the temperature of the process gas,  $C_i$  is the molar concentration of component  $i$ ,  $n_{ij}$  is the reaction order of component  $i$  in reaction  $j$ , and NC is the number of components. Similar to the reaction rate

of the thermal cracking reactions, the coking rate ( $r_c(z)$ ) can be calculated as follows:

$$r_c(z) = A_c \times e^{\frac{-E_c}{RT_c(z)}} \times C_{C_3H_6}(z) \quad (3)$$

where  $A_c$  is the pre-exponential factor for the coke formation reaction,  $E_c$  is the corresponding activation energy, and  $T_c$  is the temperature of coke surface.

$$\frac{dd_c(z)}{dt} = \frac{r_c(z)}{\varphi_c} \quad (4)$$

where  $\varphi_c$  is the coke density,  $d_c(z)$  is the coke thickness, and  $t$  is the production time.

Eqs. (2) and (3) are based on a reaction scheme proposed by Sundaram and Froment, which provides an accurate representation of the thermal cracking and coke formation processes using propane as a feedstock in the PFR [25]. According to Eqs. (2) and (3), with a fixed steam-to-propane ratio, as the reaction temperature within the PFR rises, the reaction rate increases and the cracking reactions achieve higher feedstock conversion, yielding final products with a lower average molecular weight. As one of the valuable products, propylene is both a product of the primary reaction and a reactant in secondary reactions. As the COT increases, the flow rate of the propylene outlet initially increases due to the increase in feedstock conversion; it then decreases as it undergoes secondary reactions to form products with lower molecular weight. Similar to propylene, ethylene is a reactant in secondary reactions; however, because of its greater thermodynamic stability, the temperature at which the flow rate of the ethylene outlet begins to fall is difficult to reach. As a result, the ethylene outlet flow rate is considered to increase monotonically as the COT increases within the industrial operating range. Like the rates of the cracking reactions, the coking rate increases monotonically as the temperature inside the PFR increases.

At a fixed reaction temperature, the effect of the steam-to-propane ratio can be determined using Eq. (1). An increase in the steam-to-propane ratio results in lower propane in the process gas; less feedstock is involved in the cracking reactions, so both the propylene and ethylene outlet flow rates decrease monotonically. Because of the decrease in hydrocarbon partial pressure, the rate of coking also decreases monotonically, according to Eq. (3). In addition, Eq. (4) shows that the occurrence of coking is irreversible with time.

Based on the physical information extracted from the FPM, the following physics consistency is embedded in the DM and is used as prior knowledge to increase the scalability of the model:

- With a fixed steam-to-propane ratio, the ethylene outlet flow rate and the coking rate monotonically increase, and the propylene outlet flow rate first increases and then decreases as the COT increases.
- With a fixed COT, the propylene outlet flow rate, the ethylene outlet flow rate, and the coking rate monotonically decrease as the steam-to-propane ratio increases.
- The coke layer thickness increases monotonically with time.

The accuracy of the model is guaranteed within the operating range for extracting physics consistencies, which is significantly larger than the range of the training data. However, under operating conditions beyond this common range, physics consistencies may be violated, and model scalability cannot be guaranteed. It is important to note that such extreme operating conditions are typically avoided in production. For example, in this model, the outlet flow rate of ethylene is assumed to monotonically increase with an increasing COT. However, at higher COTs, ethylene will be further cracked into methane, violating the physics consistency. In practice, such operating conditions are considered unacceptable

**Table 1**  
Configuration of a pilot-scale PFR [25].

Parameter	Value	Unit
Length of the radiant section of the PFR	95	m
Diameter of the PFR	$\phi 0.116 \times 0.008$	m
Total inlet mass flow rate	0.7635	kg·s <sup>-1</sup>
Inlet pressure	$3 \times 10^5$	Pa
Inlet temperature	873.15	K
Coke density	1600	kg·m <sup>-3</sup>
Thermal conductivity of the coke	0.00645	kJ·(m·s·K) <sup>-1</sup>

in production due to the conversion of high-value products into low-value byproducts.

### 2.2.2. Physics consistency embedding

Based on the physical information summarized in Section 2.2.1, the following equations can be given to describe the physics consistency.

With a fixed steam-to-propane ratio ( $R_{s/p}$ ),

$$\frac{\partial F_{\text{ethylene},t=n}}{\partial \text{COT}_{t=n-m}} > 0, m = 1, 2, 3, \dots, n-1 \quad (5)$$

$$\frac{\partial r_c(z)_{t=n}}{\partial \text{COT}_{t=n-m}} > 0, m = 1, 2, 3, \dots, n-1 \quad (6)$$

With a fixed COT,

$$\frac{\partial F_{\text{ethylene},t=n}}{\partial R_{s/p,t=n-m}} < 0, m = 1, 2, 3, \dots, n-1 \quad (7)$$

$$\frac{\partial F_{\text{propylene},t=n}}{\partial R_{s/p,t=n-m}} < 0, m = 1, 2, 3, \dots, n-1 \quad (8)$$

$$\frac{\partial r_c(z)_{t=n}}{\partial R_{s/p,t=n-m}} < 0, m = 1, 2, 3, \dots, n-1 \quad (9)$$

For the coke thickness,

$$\frac{dd_c(z)}{dt} > 0 \quad (10)$$

where  $n$  stands for any time step between 0 and run length.

A recurrent neural network (RNN) unit is employed in the proposed hybrid model to process inputs with physics consistency. Compared with long short-term memory (LSTM), which is often regarded as a more advanced version of RNN, the RNN avoids the need to employ the Hadamard product, thereby significantly reducing the complexity associated with ensuring physics consistency. Furthermore, RNNs have been demonstrated to sufficiently ensure physics consistency in systems with limited long-term dynamics [16,17]. Consequently, for the steam thermal cracking process, where the variables are only affected by the inputs of the previous time step, the RNN cell avoids the need for complex structural design while effectively ensuring the embedding of physics consistency. The computational process of the RNN can be expressed by the following equation:

$$h_{t=n} = \tanh(W_h h_{t=n-1} + W_x x_{t=n} + b_h + b_x) \quad (11)$$

where  $h$  is the hidden state,  $W_h$  and  $W_x$  are weighting parameters for the initial states  $h_{t=n-1}$  and inputs  $x_{t=n}$ , respectively;  $b_h$  and  $b_x$  are bias parameters of  $h_{t=n-1}$  and  $x_{t=n}$ , respectively; and  $\tanh$  is the activation function.

Thus, the following equation can express the derivative of  $h_{t=n}$  with respect to the input  $x_{t=n-m}$ .

$$\frac{\partial h_{t=n}}{\partial x_{t=n-m}} = \text{TD} \times W_h \times W_x, m = 1, 2, 3, \dots, n-1 \quad (12)$$

where TD is the product of the  $m+1$  factorials of the tanh function, which can be readily demonstrated to maintain positive values throughout its domain. To ensure positive physics consistency, the following constraints should be applied to  $W_h$  and  $W_x$ :

$$W_h > 0, W_x > 0 \quad (13)$$

For negative physics consistency,  $W_h$  and  $W_x$  follow the same constraints (Eq. (13)), but the inputs  $x_{t=n}$  need to be transformed into  $-x_{t=n}$ . In this way, all physics consistencies can be embedded in the hybrid model.

In addition to the constraints on the weighting parameters, a physics consistency term is added into the loss function to further

penalize predictions that violate physical laws. The loss function ( $L$ ) is designed as follows:

$$L = L_{\text{MSE}} + \lambda_1 L_{\text{PC}} + \lambda_2 L_{\text{REG}} \quad (14)$$

where  $L_{\text{MSE}}$  is the mean square error loss;  $L_{\text{PC}}$  is the physics inconsistency loss; and  $L_{\text{REG}}$  represents the regularization loss, which is introduced to mitigate the risk of model overfitting.  $\lambda_1$  and  $\lambda_2$  are weighting factors that regulate the relative importance of each loss term. Up to this point, physics consistency is ensured in the PCML-based hybrid model.

### 2.2.3. Sub-models in DM

Three sub-models—namely, a model of the outlet flow rates of the valuable products, a coke formation model, and an energy consumption model—were built through PCML-based HM. By embedding the physics consistency extracted from the FPM, the DM is used to find mathematical relationships between the inputs and outputs. The DM works as a surrogate model and was implemented on Python® 3.8 with the Pytorch® 1.10.1 deep learning framework.

(1) **Model of the outlet flow rates of valuable products.** Considering the capacity of the thermal cracking furnace, the total mass flow rate of the process gas is set to a fixed value of  $0.7635 \text{ kg}\cdot\text{s}^{-1}$ . Therefore, the flow rate of propane can be calculated according to the steam-to-propane ratio. In order to evaluate the economic efficiency of the thermal cracking furnace, it is necessary to calculate the outlet flow of valuable products at the PFR outlet. According to the rate law, the rates of the cracking reactions are mainly determined by the reaction temperature and the concentration of the reactants, which correspond to the operating variables—the COT, the steam-to-propane ratio, and the state variables  $d_c(z)$ . Therefore, the outlet flow rates of valuable products can be calculated as follows:

$$F_{\text{ethylene},t=n} = f(\text{COT}, R_{s/p}, d_c(z=95))_{t=n} \quad (15)$$

$$F_{\text{propylene},t=n} = f(\text{COT}, R_{s/p}, d_c(z=95))_{t=n} \quad (16)$$

where  $d_c(z=95)$  is the coke thickness at the PFR outlet.

(2) **Coke formation model.** In the operational cycle of a thermal cracking furnace, coke formation plays a crucial role, affecting not only the cracking reactions and heat transfer during operation but also the run length of the PFR and the frequency of coke clearing throughout the cycle. The coking rate, similar to the thermal cracking reactions, is determined by the temperature of the coke surface and the concentration of the coke precursor (propylene), according to the rate law. The coke layer continuously accumulates, and its thickness is determined by the coking rate at the current time step and the coke layer thickness at the previous time step, which can be expressed by the following equations:

$$r_c(z)_{t=n} = f(\text{COT}, R_{s/p}, d_c(z=95))_{t=n} \quad (17)$$

$$d_c(z)_{t=n+1} = f(d_c(z), r_c(z))_{t=n} \quad (18)$$

(3) **Energy consumption model.** The energy consumption of the PFR in a thermal cracking furnace mainly stems from the heating of the process gas and the heating of reaction. Thus, the energy consumption is affected by the COT, the steam-to-diluent ratio, and the coke thickness. In their studies, Yu et al. [12] and Zhao et al. [26] used a polynomial regression of the COT, steam-to-propane ratio, and process gas flow rate to calculate the energy consumption. In this study, the dynamic impact of varying coke thicknesses is taken into account, so the energy consumption ( $Q$ ) can be obtained by the following equation:

$$Q_{t=n} = f(\text{COT}, R_{s/p}, d_c(z = 95))_{t=n} \quad (19)$$

### 2.3. Model validation

A total of 170 sets of dynamic data (70% training set plus 30% test set) obtained from the validated FPM were used to train and test the accuracy of the DM. The steam-to-propane ratio and the COT, as the most sensitive operating variables, varied over the following operating range:

- Steam-to-propane ratio: 0.2–1.0 kg·kg<sup>-1</sup>.
- COT: 973.15–1143.15 K.

Each set of data was obtained by running the FPM of the PFR from clean tube conditions to shutdown under one of the operating conditions within the above operating ranges. The data index of one set of data depended on the run length of the PFR under the given operating conditions (each data index was collected with a time interval of 10 h). The predicted results for each sub-model used for the multi-objective optimization were compared with the values obtained from FPM. The outputs from an artificial neural network (ANN) without physics consistency using the same input were compared with the outputs from PCML. The root mean square error (RMSE), mean absolute percentage error (MAPE), and coefficient of determination ( $R^2$ ) were selected as key metrics to quantitatively evaluate the accuracy, relative error, and data interpretation abilities of the PCML and ANN.

As shown in Fig. 2, PCML has a higher accuracy than the ANN on the test set, and the PCML-based hybrid model can accurately predict the flow rate of valuable products, the impact of coke formation, the run length of the PFR, and the total energy consumption. Table 2 shows that the PCML-based hybrid model demonstrates superior performance over the ANN model, as indicated by its higher  $R^2$  value and lower RMSE and MAPE values. These results suggest that the PCML-based hybrid model outperforms the ANN in both model accuracy and data interpretation capability. The enhanced performance can be attributed to the

physics consistency embedding, which effectively captures the dynamic long-term variation trends of output variables by controlling error accumulation. Particularly for predicting variables such as the coking rate, which are highly sensitive to dynamic changes in input variables, the model requires enhanced capability in long-term prediction to ensure accurate and reliable results. In predicting the coking rate, the PCML-based hybrid model achieved a significantly higher  $R^2$  value of 0.9845 compared with the ANN's 0.4940.

### 3. Multi-objective optimization

Based on the PCML-based hybrid model developed in Section 2, a multi-objective optimization framework for a thermal cracking furnace is proposed, whose structure is shown in Fig. 3. The optimization framework takes the annual profit and annual CO<sub>2</sub> emissions as the optimization objectives and aims to optimize the economic benefit and environmental impact at the same time. A non-dominated sorting genetic algorithm II (NSGA-II) is used to solve the multi-objective dynamic optimization problem.

#### 3.1. Objectives functions

As shown in Fig. 1, a typical operational cycle starts with clean tube conditions, continues with coke formation until shutdown, and then requires 48 h for decoking before restarting from clean tube conditions. For economic benefits, ethylene and propylene can be sold as valuable products; their total production in an operational cycle can be calculated from the following equations:

$$F_{\text{ethylene, total}} = \sum_{t=0}^{t_c} F_{\text{ethylene, } t} \Delta t_i \quad (20)$$

$$F_{\text{propylene, total}} = \sum_{t=0}^{t_c} F_{\text{propylene, } t} \Delta t_i \quad (21)$$

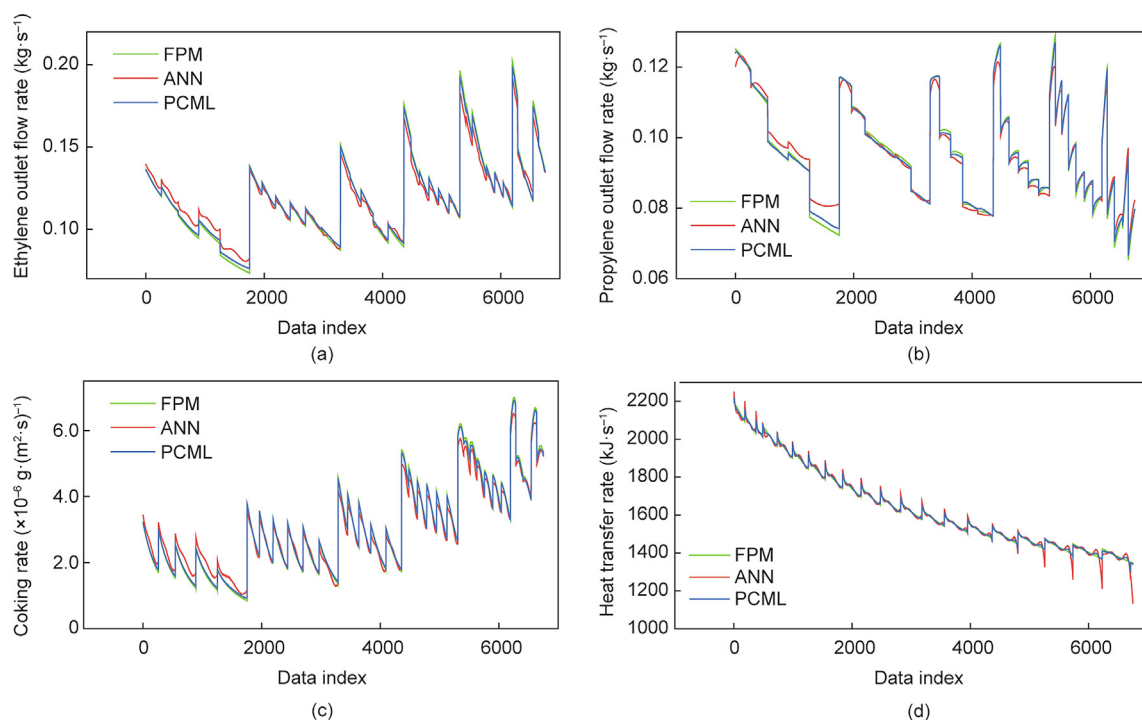
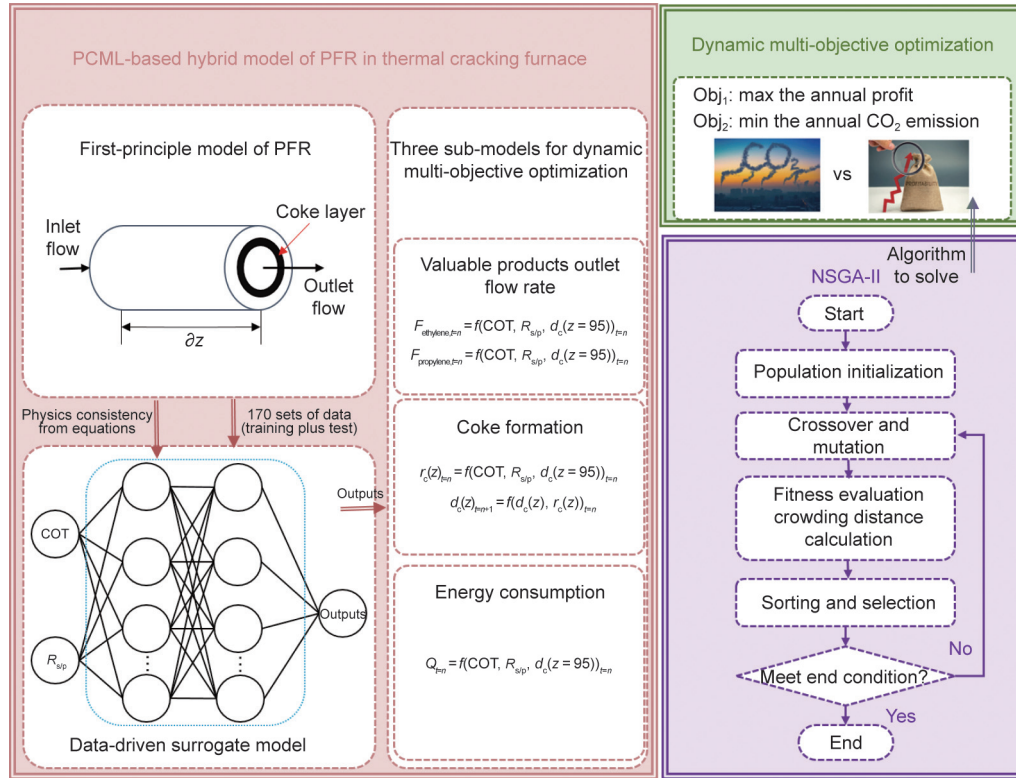


Fig. 2. Comparisons of the outputs of the PCML and ANN models on the test set. (a) Ethylene outlet flow rate; (b) propylene outlet flow rate; (c) coking rate at the PFR outlet; (d) heat transfer rate.

**Table 2**  
Comparison of prediction performance of ANN versus PCML.

Metric	Ethylene outlet flow rate		Propylene outlet flow rate		Coking rate		Heat transfer rate	
	ANN	PCML	ANN	PCML	ANN	PCML	ANN	PCML
RMSE <sup>a</sup>	$3.75 \times 10^{-3}$	$1.11 \times 10^{-4}$	$4.27 \times 10^{-3}$	$7.21 \times 10^{-5}$	$5.15 \times 10^{-7}$	$1.68 \times 10^{-8}$	$6.38 \times 10^{-4}$	$2.33 \times 10^{-5}$
MAPE	2.3400%	0.0511%	2.1500%	0.0633%	4.6100%	0.2130%	3.7800%	0.0589%
R <sup>2</sup>	0.8884	0.9927	0.8932	0.9876	0.4940	0.9845	0.8876	0.9971

<sup>a</sup> The units of RMSE values are the same as those of the original data.



**Fig. 3.** Framework of the multi-objective optimization. NSGA-II: non-dominated sorting genetic algorithm II.

where  $t_c$  is the run length of the PFR—that is, the time from clean tube conditions to when the coke layer reaches 0.0135 m—and  $\Delta t_i$  is the reporting time interval of the model. Since there is only a small change in coke thickness within 1 h,  $\Delta t_i$  is chosen to be 10 h.

The cost during production time mainly comes from the purchasing of the feedstock propane, diluent, and energy. Since the total mass flow rate of the inlet process gas is fixed at 0.7635 kg·s<sup>-1</sup>, the mass flow rates of the propane and steam used in an operational cycle can be calculated by the following equations.

$$F_{\text{propane, total}} = \sum_{t=0}^{t_c} \left( 0.7635 \times \frac{1}{1 + R_{s/p,t}} \right) \Delta t_i \quad (22)$$

$$F_{\text{steam, total}} = \sum_{t=0}^{t_c} \left( 0.7635 \times \frac{R_{s/p,t}}{1 + R_{s/p,t}} \right) \Delta t_i \quad (23)$$

The cost of energy during the run length can be calculated by the following equation:

$$Q_{\text{total}} = \sum_{t=0}^{t_c} Q_t \Delta t_i \quad (24)$$

The economic loss caused by the decoking process consists of the production loss from downtime and the fixed decoking cost (DCC). The number of operational cycles per year ( $N_{\text{cycle}}$ ) can be cal-

culated by means of the following equation to evaluate the effect of decoking frequency:

$$N_{\text{cycle}} = \frac{8760}{t_c + t_d} \quad (25)$$

where  $t_d$  is the time for decoking.

The CO<sub>2</sub> emissions during the production time ( $E_p$ ) of the thermal cracking furnace are mainly caused by the combustion of fuel and can be calculated by the following equations:

$$Q_{\text{total}} = m_{\text{fuel}} \times H_{\text{fuel}} \quad (26)$$

$$E_p = m_{\text{fuel}} \times E_{\text{fuel}} \quad (27)$$

where  $m_{\text{fuel}}$  is the mass of fuel consumed to produce energy,  $H_{\text{fuel}}$  is the heat value of the fuel, and  $E_{\text{fuel}}$  represents the CO<sub>2</sub> emissions from burning the fuel.

During the decoking process, the CO<sub>2</sub> emissions mainly come from the energy consumed to heat the steam–air mixture and the CO<sub>2</sub> generated directly from the coke combustion. Burners in the thermal cracking furnace typically burn about 33% of the fuel used to heat the steam–air mixture during the coke decoking process [21]. In this study, we take 33% of the average CO<sub>2</sub> emission rate ( $E_{f, \text{basecase}}$ ) over the production time of the working conditions ( $t_{c, \text{basecase}}$ ) typically used in industry (COT: 1113.15 K;

steam-to-propane ratio: 0.4) to represent the CO<sub>2</sub> produced by the decoking process from energy consumption ( $E_{df}$ ):

$$E_{df} = \frac{1}{3} \times \frac{E_{f,basecase}}{t_{c,basecase}} \quad (28)$$

The distribution of the thickness of the coke layer along the tube inner wall can be calculated using Eq. (18), and then the CO<sub>2</sub> generated from the direct combustion of coke during the decoking process ( $E_{dc}$ ) can be determined by the following equation:

$$E_{dc} = \sum_{z=0}^{95} \frac{\varphi_c d_c(z) A_z}{M_{wC}} M_{wCO_2} \quad (29)$$

where  $A_z$  is the area of the inner tube wall surface for each differential element,  $M_{wC}$  is the molecular weight of carbon, and  $M_{wCO_2}$  is the molecular weight of CO<sub>2</sub>.

Therefore, the CO<sub>2</sub> emissions during the decoking process ( $E_d$ ) can be calculated:

$$E_d = E_{df} + E_{dc} \quad (30)$$

Based on the sub-models developed in Section 2.2.2, the following objective functions can be formed:

Maximize annual profit:

$$P_{annual} = \left[ (F_{ethylene,total} \times COS_{ethylene} + F_{propylene,total} \times COS_{propylene}) - (F_{propane,total} \times COS_{propane} + F_{steam,total} \times COS_{steam} + m_{fuel} \times COS_{fuel} + DCC) \right] \times N_{cycle} \quad (31)$$

where COS represents the price factors of different components.

Minimize annual CO<sub>2</sub> emissions:

$$E_{annual} = (E_p + E_d) \times N_{cycle} \quad (32)$$

The parameters from previous studies [10,11] that are listed in Table 3 can be used for the multi-objective optimization.

### 3.2. Decision variables and constraints

#### 3.2.1. Sensitivity analysis of decision variables

The COT and the steam-to-propane ratio are used as the decision variables in this study. To analyze their impacts on the results of the multi-objective optimization and to determine whether physics consistencies are followed, a sensitivity analysis based on the results of the PCML-based hybrid model was carried out to examine the influence of the COT and steam-to-propane ratio on key performance indicators. The results of the sensitivity analysis are presented in Fig. 4.

According to Fig. 4(a), increasing the COT increases the propane conversion rate, which increases the annual profit. However, it should be noted that the impact of a higher propane conversion rate is not always positive, as this involves a critical trade-off between the outlet flow rates of ethylene and propylene. Fig. 4(b) indicates that increasing the COT leads to a shorter run length of the thermal cracking furnace and increased energy consumption, both of which have negative impacts on the annual profit and annual CO<sub>2</sub> emissions.

**Table 3**  
Parameters for the multi-objective optimization.

Parameter	Physical meaning	Value	Unit
$t_d$	Decoking time per cycle	48	h
$COS_{propane}$	Propane price factor	0.596	USD·kg <sup>-1</sup>
$COS_{ethylene}$	Ethylene price factor	1.356	USD·kg <sup>-1</sup>
$COS_{propylene}$	Propylene price factor	1.576	USD·kg <sup>-1</sup>
$COS_{steam}$	Steam price factor	0.0129	USD·kg <sup>-1</sup>
$COS_{fuel}$	Fuel price factor	0.056	USD·kg <sup>-1</sup>
DCC	Decoking cost per cycle	66 000	USD

Fig. 4(c) demonstrates that increasing the steam-to-propane ratio results in a decreased propane conversion rate and lower outlet flow rates of ethylene and propylene, both of which are undesirable when considering the annual profit. Nevertheless, as illustrated in Fig. 4(d), both the extended run length of the thermal cracking furnace and the reduced energy consumption associated with higher steam-to-propane ratios can increase the annual profit and reduce the annual CO<sub>2</sub> emissions.

In summary, the PCML-based hybrid model's predictions align with the physics consistencies. In addition, the results for both the COT and the steam-to-propane ratio show that they have significant and complex influences on the annual profit and annual CO<sub>2</sub> emissions, justifying their selection as the decision variables for the multi-objective dynamic optimization. Based on the results of the sensitivity analysis, the decision variables were discretized within reasonable intervals during the optimization process to reduce the computational demand. The discretization interval was set at 5 K for COT and at 0.01 for the steam-to-propane ratio.

#### 3.2.2. Constraints

The following common operating ranges will be used as constraints [27]:

$$973 \text{ K} < \text{COT} < 1143 \text{ K} \quad (33)$$

$$0.2 < R_{s/p} < 1.0 \quad (34)$$

Considering the wear and tear on the thermal cracking furnace caused by too-frequent decoking, the third constraint is that the run length of the thermal cracking furnace should not be less than the minimum run length ( $t_{c,min}$ ) [28]:

$$t_c \geq t_{c,min} \quad (35)$$

Here,  $t_{c,min}$  is largely determined by the specific type of thermal cracking furnace and feedstock type. As presented in Fig. 4, the operating conditions with a high COT and low steam-to-propane ratio result in an extremely short run length. Shorter run length operating conditions have higher propane conversion rates and higher annual CO<sub>2</sub> emissions. However, the annual profit is not only determined by the propane conversion rate but also depends on other trade-offs. In this study,  $t_{c,min}$  was set to 28 days (672 h). Increasing  $t_{c,min}$  does not affect the Pareto front, as operating conditions failing to meet this constraint ( $t_{c,min} = 672 \text{ h}$ ) are typically dominated by solutions on the Pareto front due to their higher energy consumption, reduced propylene outlet flow rate, and frequent shutdown. However, if  $t_{c,min}$  is reduced due to requirements such as equipment maintenance, some solutions near the anchor point of the Pareto front with maximum annual profit will be eliminated or replaced, while solutions approaching the anchor point of minimum annual CO<sub>2</sub> emissions will remain unaffected.

### 3.3. Non-dominated sorting genetic algorithm II

#### 3.3.1. Steps for NSGA-II

The NSGA-II is a well-established multi-objective optimization algorithm that utilizes non-dominated sorting and crowding distance mechanisms to ensure both population diversity and convergence toward the Pareto optimal solution [29]. As shown in Fig. 3, the procedure of this algorithm is presented below:

**Step 1:** Start by randomly generating an initial population of size  $N$ , ensuring that the individuals meet the predefined operating constraints.

**Step 2:** Create an offspring population also of size  $N$ , through genetic algorithm operations—selection, crossover, and mutation.

**Step 3:** Perform fast non-dominated sorting on the individuals in the initial population and calculate the crowding distance for

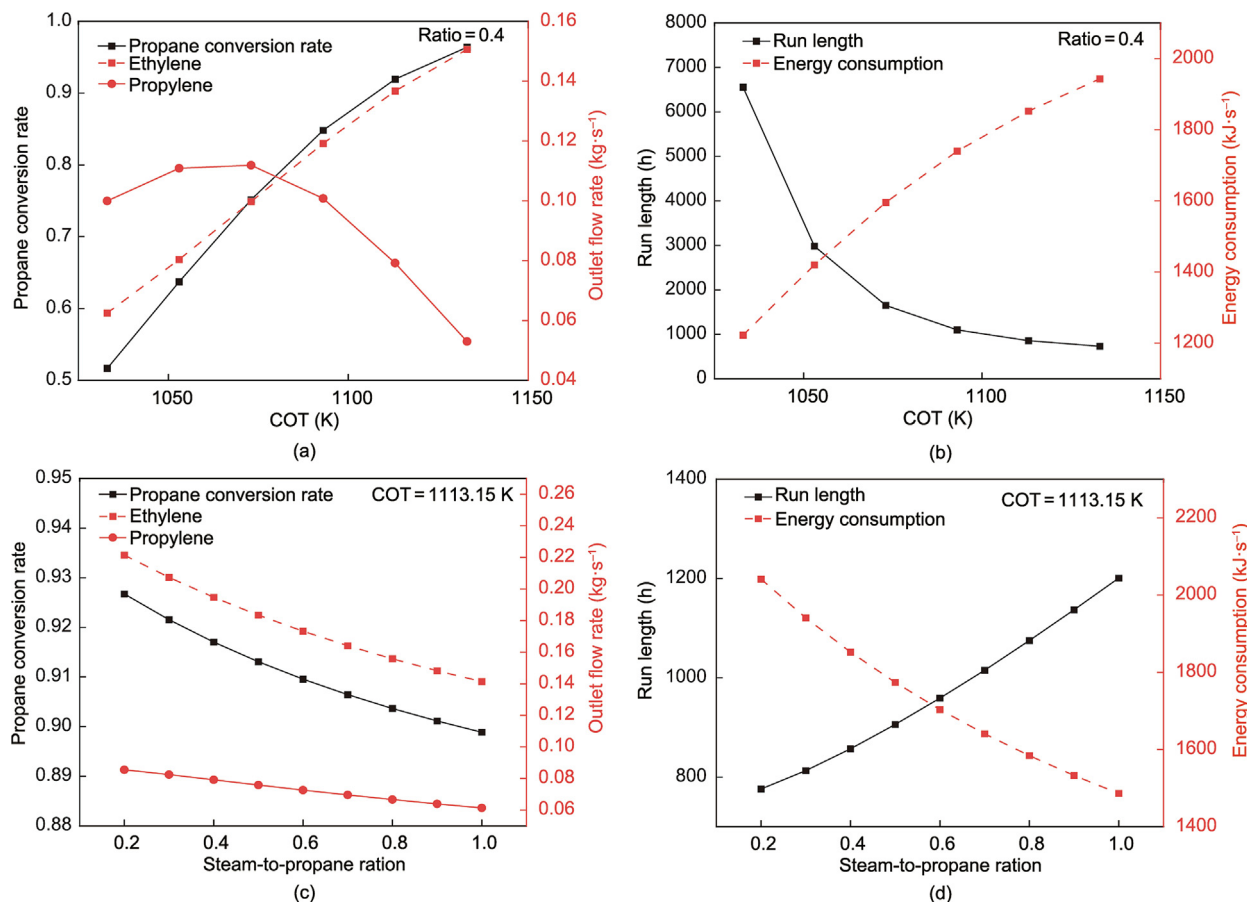


Fig. 4. Sensitivity analysis of the (a, b) COT and (c, d) steam-to-propane ratio.

the individuals within each dominance layer. Then, perform tournament selection based on the calculated crowding distance to choose  $M$  suitable individuals from the initial population to form the new population.

**Step 4:** Return to step 2 and repeat the above process until the termination condition is met.

**Step 5:** Once the termination condition is satisfied, the algorithm ends, and the optimal solution set is output.

### 3.3.2. Parameters for NSGA-II

According to the steps outlined in Section 3.3.1, the implementation of NSGA-II requires the selection of several key parameters, including population size, number of generations (termination condition), crossover probability, and mutation probability. The selection of these parameters significantly influences both the convergence of the optimization results and the computational efficiency. More specifically, while increasing the population size increases the diversity of the optimization results, it also increases the computational demands [30]. Similarly, an insufficient number of generations may prevent the algorithm from converging, whereas an excessive number increases the computational demand without significantly improving the solution quality [31]. The selection of crossover and mutation probabilities also involves a trade-off between convergence and computational demand. The range of these parameters is determined by the complexity of the optimization problem, such as the number of decision variables, the number of objective functions, the number of constraints, and the nonlinearity of the objective functions. Several studies focusing on optimization algorithms have employed various algorithms to determine the true Pareto front, using it as a

benchmark to set these parameters of NSGA-II [32–34]. In this study, since NSGA-II is solely employed to address the optimization problem, the true Pareto front remains unknown. Consequently, the adopted methodology involves identifying NSGA-II parameter ranges in existing works in the literature that address problems of a similar complexity using NSGA-II [13,35,36]. Within the determined parameter range, this method involves testing from lower-computational-cost settings with potentially weaker solving capabilities to higher-computational-cost settings with better solving capabilities, until further increases in parameter values only increase the computational costs without significantly improving the optimization results. The parameter ranges and values used in this study are presented in Table 4 [13,35,36].

## 4. Results and discussion

The multi-objective dynamic optimization based on a PCML-based hybrid model was carried out on a personal computer with an Intel Core i7-6700 central processing unit (CPU) and 128 GB random access memory (RAM). As shown in Table 5, the

Table 4  
Parameters for NSGA-II.

Parameter	Range [13,35,36]	Value used in this study
Population size	30–300	200
Number of generation	50–200	100
Crossover probability	0.8–0.9	0.85
Mutation probability	0.10–0.33	0.15

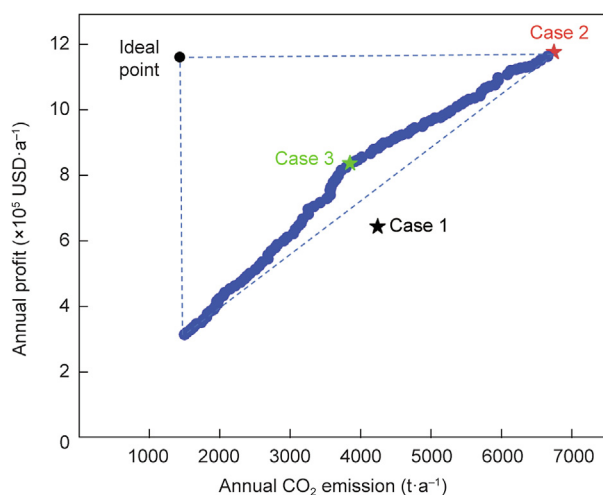
**Table 5**

Comparison of the computational efficiency of this study versus that of an existing work.

Item	PCML-based hybrid model used in this study	FPM used in existing work [37]
Computational device	Intel Core i7-6700, 128 GB RAM	Dual core, 3 GB RAM
Computational demand	77 s	19 h
Optimization complexity	Multi-objective dynamic	Single-objective dynamic
Time interval	10 h	24 h

computational demand of this multi-objective optimization was 77 s, which is significantly lower than the dynamic optimization based on FPM alone in an existing work [37]. It should be noted that the time interval used in this study was 10 h. Compared with the previous work, which used a 24 h time interval, the optimization problem formulated in this work is more challenging. HM significantly increases the computational efficiency of complex optimization problems, and such an approach can be applied to other complex systems and processes. However, it is worth noting that the formation of coke is relatively slow in the steam cracking process, so the model exhibits pseudo-dynamic characteristics. For processes with more complex dynamic properties, the development of hybrid models and the embedding of physics consistencies will present greater challenges.

The Pareto front of this multi-objective optimization is shown in Fig. 5, where each point on the figure represents a set of optimized operating variables that change over time. In an ideal scenario, the two objective functions would simultaneously achieve their optimal values. However, such an ideal state is practically unattainable. The multi-objective optimal operating condition is defined as the point closest to the ideal point while the distance between each solution point and the ideal point is calculated using normalized values [38]. In order to assess the effects of the multi-

**Fig. 5.** Pareto front of the multi-objective optimization.**Table 6**

Results of the multi-objective optimization.

Case	Annual profit (USD·a <sup>-1</sup> )	Annual CO <sub>2</sub> emissions (t·a <sup>-1</sup> )	Run length (h)	Operational cycle per year
Case 1	642 060	4 241	857	10.2
Case 2	1 177 110	6 741	722	12.1
Case 3	836 016	3 850	872	10.0

objective dynamic optimization regarding the trade-off between profit and CO<sub>2</sub> emissions for green ethylene manufacturing, three cases were compared: the base case commonly used in the industry, with given operating variables (case 1); highest-profit operating conditions (case 2); and the multi-objective optimal operating conditions (case 3).

As shown in Table 6, the fixed operating conditions of case 1 (COT: 1113.15 K; steam-to-propane ratio: 0.4) are far worse than the optimal operating conditions on the Pareto front in terms of both profit and CO<sub>2</sub> emissions. Therefore, dynamically adjusting the operating variables according to the growth of the coke thickness can effectively increase the profit and reduce CO<sub>2</sub> emissions. In addition, the optimization strategy successfully balances two objectives. Compared with case 2, case 3 sacrifices an annual profit of 341 094 USD·a<sup>-1</sup> (28.98%) for a CO<sub>2</sub> emission reduction of 2891 t (42.89%). Case 3, which has more environmentally friendly operating conditions, has a longer PFR run length and lower decoking frequency.

The operating variables from clean tube conditions to shutdown conditions are shown in Fig. 6, which shows that the trends of the two operating variables along the production time are similar in cases 2 and 3. As the coke thickness increases, the effective reaction volume within the PFR diminishes, leading to a decrease in feedstock conversion rates and reduced yields of valuable products. Therefore, the reaction rate of the cracking reaction must be maintained by increasing the COT, which is shown in Fig. 6(a). As shown in Fig. 6(b), the optimal operating conditions in cases 2 and 3 both suggest that the steam-to-propane ratio is gently increased and then slowly decreased. Since the reaction rates of thermal cracking must be maintained by increasing the COT, which significantly increases the coking rate, this needs to be compensated for by increasing the steam-to-propane ratio in the first half of the production time to prevent the economic losses and environmental impacts caused by frequent shutdown for decoking. However, as the COT continues to rise, the profit caused by extending the PFR run length by increasing the steam-to-propane ratio is no longer significant, so the multi-objective optimal operating condition suggests reducing the steam-to-propane ratio to increase the propane mass flow rate in the process gas until the shutdown conditions are met. Although the trends of the operating variables with production time are similar for cases 2 and 3, in case 2, the PFR always runs at a higher COT and lower steam-to-propane ratio compared with case 3. This is because case 2 has optimal-profit operating conditions for the entire operational cycle. Although the economic loss of shutdown is taken into account, the environmental impact is ignored. Thus, case 2 suggests that the PFR should use a higher process gas temperature (higher COT) and more propane (lower steam-to-propane ratio) to participate in the reaction. As shown in Fig. 7, case 2 has a higher ethylene outlet flow rate and a similar propylene outlet flow rate compared with case 3 during the production times. However, case 2 has a much higher coking rate than case 3 (shown in Fig. 7(c)), resulting in a 150 h (17.2%) reduction in the run length of the PFR in case 2.

As discussed earlier, although case 3 sacrifices some of the annual profit, it exhibits a notable reduction in the annual CO<sub>2</sub> emissions. Fig. 8 shows that the CO<sub>2</sub> emissions for both the production time and the decoking process are reduced in case 3 compared

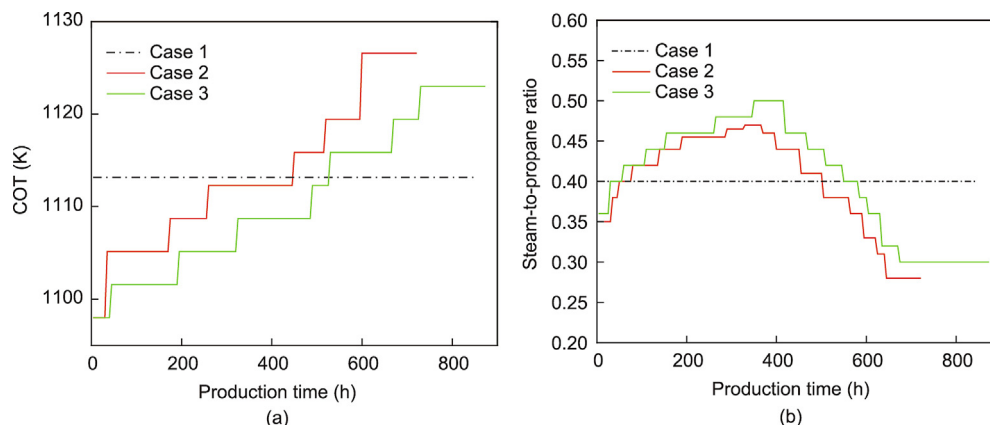


Fig. 6. Comparisons of the operating variables along the production time. (a) COT; (b) steam-to-propane ratio.

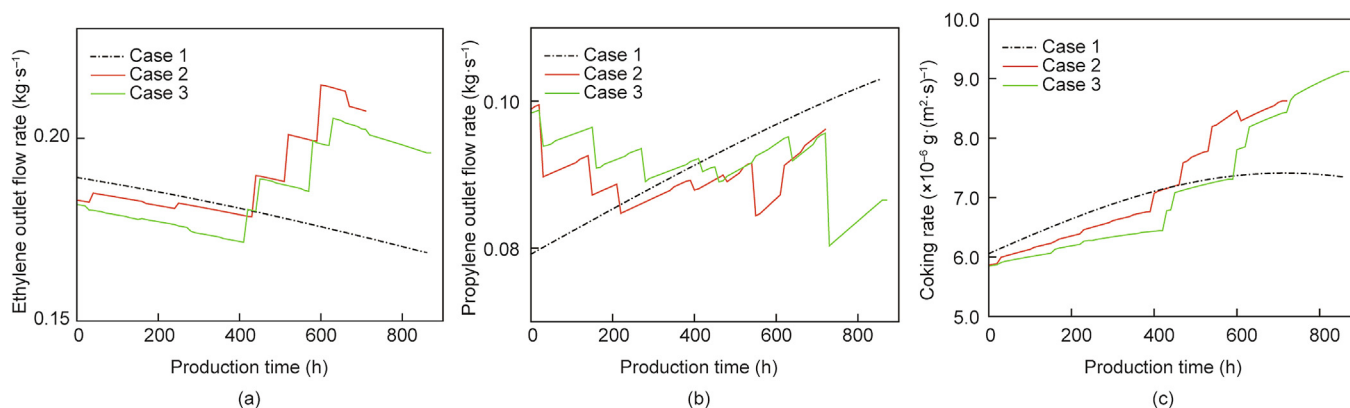


Fig. 7. Comparisons of (a) the ethylene outlet flow rate, (b) the propylene outlet flow rate, and (c) the coking rates of the three cases.

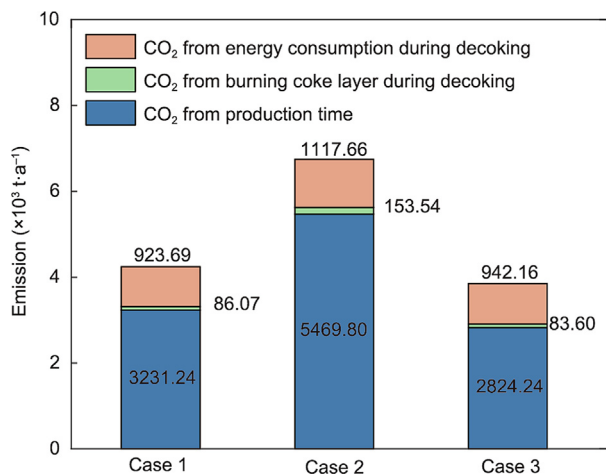


Fig. 8. Comparison of CO<sub>2</sub> emissions during whole operational cycles of three cases.

with case 2. During the production time, case 3 reduces CO<sub>2</sub> emissions through less energy-intensive operating conditions (lower COT, higher steam-to-propane ratio). The reduction in CO<sub>2</sub> emissions during the decoking process is achieved by increasing the run length of the PFR to obtain a lower decoking frequency. A comparison of the CO<sub>2</sub> reductions of case 3 and case 2 over the whole operational cycle shows that the emission reduction during the run length (91.5%) is more significant than the emission reduction during the decoking process (8.5%). Therefore, the dynamic optimization

and adjustment of the operating variables mainly affect the energy consumption during operation and thus reduce emissions. Although the impact of the decoking process is reduced by extending the PFR run length, this part of the emission reduction is limited by existing decoking technology.

### 5. Conclusions

In this paper, a novel PCML-based hybrid model was developed to carry out multi-objective dynamic optimization for the operation of a thermal cracking furnace in order to promote green ethylene manufacturing. The accuracy and scalability of the newly developed hybrid model were improved by extracting the physical information in the FPM and embedding it as physics consistency in the training of the DM. The hybrid model significantly reduced the computational demand for the multi-objective dynamic optimization to 77 s. The results of the optimization showed that dynamically adjusting the operating variables with coke formation can effectively improve profit and reduce CO<sub>2</sub> emissions. This study indicates that sacrificing 28.97% of the annual profit can significantly reduce the annual CO<sub>2</sub> emissions by 42.89%. During the production time, reducing CO<sub>2</sub> emissions is mainly done by operating under lower-energy-consuming conditions; for the decoking process, carbon emissions are mainly reduced by increasing the run length of the PFR.

This study proposes the green production of ethylene through an AI approach. Future studies can focus on the following key areas: Firstly, the HM approach proposed in this study can be extended to other complex industrial processes to achieve

advanced applications in design, optimization, and control. Secondly, significant attention should be devoted to the decarbonization of decoking technology, which holds significant potential for advancing green manufacturing. For existing decoking technologies, the flue gas generated from coke combustion contains a considerable amount of thermal energy. Therefore, exploring the recovery and reuse of this waste heat could significantly increase the thermal efficiency of the decoking process. Additionally, the feasibility of integrating clean energy sources to partially replace the energy consumption of the decoking process should be evaluated, thereby promoting the decarbonization of decoking technology.

### CRedit authorship contribution statement

**Yao Zhang:** Writing – original draft, Methodology, Software, Writing – review & editing, Conceptualization, Validation. **Peng Sha:** Software, Methodology, Writing – review & editing. **Meihong Wang:** Writing – review & editing, Funding acquisition, Conceptualization, Supervision. **Cheng Zheng:** Software, Writing – review & editing, Methodology. **Shengyuan Huang:** Software, Writing – review & editing. **Xiao Wu:** Supervision, Funding acquisition. **Joan Cordiner:** Writing – review & editing, Supervision.

### Declaration of competing interest

The authors declare that they have no known competing financial interests or personal relationships that could have appeared to influence the work reported in this paper.

### Acknowledgments

The authors would like to acknowledge the financial support of the National Key Research and Development Program of China (2021YFE0112800) and EU RISE project OPTIMAL (101007963).

### References

- [1] Sadrameli S. Thermal/catalytic cracking of hydrocarbons for the production of olefins: a state-of-the-art review I: thermal cracking review. *Fuel* 2015;140:102–15.
- [2] Fakhroleslam M, Sadrameli SM. Thermal cracking of hydrocarbons for the production of light olefins; a review on optimal process design, operation, and control. *Ind Eng Chem Res* 2020;59(27):12288–303.
- [3] Yuan B, Zhang Y, Du W, Wang M, Qian F. Assessment of energy saving potential of an industrial ethylene cracking furnace using advanced exergy analysis. *Appl Energy* 2019;254:113583.
- [4] Hu G, Li X, Liu X, Hu J, Otitoju O, Wang M, et al. Techno-economic evaluation of post-combustion carbon capture based on chemical absorption for the thermal cracking furnace in ethylene manufacturing. *Fuel* 2023;331:125604.
- [5] Li Z, Ahman M, Nilsson LJ, Bauer F. Towards carbon neutrality: transition pathways for the Chinese ethylene industry. *Renew Sustain Energy Rev* 2024;199:114540.
- [6] Zhang Y, Vangaever S, Theis G, Henneke M, Heynderickx GJ, Van Geem KM. Feasibility of biogas and oxy-fuel combustion in steam cracking furnaces: experimental and computational study. *Fuel* 2021;304:121393.
- [7] Tijani M, Zondag H, Van Delft Y. Review of electric cracking of hydrocarbons. *ACS Sustain Chem Eng* 2022;10(49):16070–89.
- [8] Amghizar I, Dedeyne JN, Brown DJ, Marin GB, Van Geem KM. Sustainable innovations in steam cracking: CO<sub>2</sub> neutral olefin production. *React Chem Eng* 2020;5(2):239–57.
- [9] Masoumi ME, Sadrameli SM, Towfighi J, Niaei A. Simulation, optimization and control of a thermal cracking furnace. *Energy* 2006;31(4):516–27.
- [10] Gao GY, Wang M, Ramshaw C, Li XG, Yeung H. Optimal operation of tubular reactors for naphtha cracking by numerical simulation. *Asia Pac J Chem Eng* 2009;4(6):885–92.
- [11] Berreni M, Wang M. Modelling and dynamic optimization of thermal cracking of propane for ethylene manufacturing. *Comput Chem Eng* 2011;35(12):2876–85.
- [12] Yu K, While L, Reynolds M, Wang X, Liang JJ, Zhao L, et al. Multiobjective optimization of ethylene cracking furnace system using self-adaptive multiobjective teaching-learning-based optimization. *Energy* 2018;148:469–81.
- [13] Shen W, Tian Z, Zhao L, Qian F. Life cycle assessment and multiobjective optimization for steam cracking process in ethylene plant. *ACS Omega* 2022;7(18):15507–17.
- [14] Zendejboudi S, Rezaei N, Lohi A. Applications of hybrid models in chemical, petroleum, and energy systems: a systematic review. *Appl Energy* 2018;228:2539–66.
- [15] Rezaei N, Rahimpour MR, Khayatian A, Jahanmiri A. A new hybrid approach in the estimation of end-states of a tubular plug-flow reactor by Kalman filter. *Chem Eng Process* 2008;47(5):770–9.
- [16] Bui L, Joswiak M, Castillo I, Phillips A, Yang J, Hickman D. A hybrid modeling approach for catalyst monitoring and lifetime prediction. *ACS Eng Au* 2022;2(1):17–26.
- [17] Xiao T, You F. Building thermal modeling and model predictive control with physically consistent deep learning for decarbonization and energy optimization. *Appl Energy* 2023;342:121165.
- [18] Xiao T, You F. Physically consistent deep learning-based day-ahead energy dispatching and thermal comfort control for grid-interactive communities. *Appl Energy* 2024;353:122133.
- [19] Ren T, Patel MK, Blok K. Steam cracking and methane to olefins: energy use, CO<sub>2</sub> emissions and production costs. *Energy* 2008;33(5):817–33.
- [20] Fakhroleslam M, Sadrameli SM. Thermal/catalytic cracking of hydrocarbons for the production of olefins; a state-of-the-art review III: process modeling and simulation. *Fuel* 2019;252:553–66.
- [21] Mynko O, Amghizar I, Brown DJ, Chen L, Marin GB, de Alvarenga RF, et al. Reducing CO<sub>2</sub> emissions of existing ethylene plants: evaluation of different revamp strategies to reduce global CO<sub>2</sub> emission by 100 million tonnes. *J Clean Prod* 2022;362:132127.
- [22] Sarris SA, Symoens SH, Olahova N, Reyniers MF, Marin GB, Van Geem KM. Alumina-based coating for coke reduction in steam crackers. *Materials* 2020;13(9):2025.
- [23] Zhang Y, Yan H, Chong D, Cordiner J, Wang M. Modelling, simulation, exergy and economic analyses of thermal cracking of propane using CO<sub>2</sub> and steam as diluents. *Comput Aided Chem Eng* 2024;53:691–6.
- [24] Zhang Y, Yan H, Chong D, Guo C, Huang S, Cordiner J, et al. Modelling, simulation, thermodynamic and economic performance analysis of steam and CO<sub>2</sub> as diluents in thermal cracking furnace for ethylene manufacturing. *Fuel* 2025;381:133656.
- [25] Sundaram K, Froment G. Kinetics of coke deposition in the thermal cracking of propane. *Chem Eng Sci* 1979;34(5):635–44.
- [26] Zhao H, Ierapetritou MG, Rong G. Production planning optimization of an ethylene plant considering process operation and energy utilization. *Comput Chem Eng* 2016;87:1–12.
- [27] Van Damme P, Narayanan S, Froment G. Thermal cracking of propane and propane-propylene mixtures: pilot plant versus industrial data. *AIChE J* 1975;21(6):1065–73.
- [28] Cui Y, Han Y, Geng Z, Zhu Q, Fan J. Production optimization and energy saving of complex chemical processes using novel competing evolutionary membrane algorithm: emphasis on ethylene cracking. *Energy Conver Manage* 2019;196:311–9.
- [29] Bhaskar V, Gupta SK, Ray AK. Applications of multiobjective optimization in chemical engineering. *Rev Chem Eng* 2000;16(1):1–54.
- [30] Deb K, Pratap A, Agarwal S, Meyarivan TA. A fast and elitist multiobjective genetic algorithm: NSGA-II. *IEEE Trans Evol Comput* 2002;6(2):182–97.
- [31] Hamdani TM, Won JM, Alimi AM, Karray F. Multi-objective feature selection with NSGA-II. In: Beliczynski B, Dzielinski A, Iwanowski M, Ribeiro B, editors. *Proceedings of the 8th International Conference on Adaptive and Natural Computing Algorithms*; 2007 Apr 11–14; Warsaw, Poland. Berlin: Springer; 2007. p. 240–7.
- [32] Xu XF, Wang K, Ma WH, Wu CL, Huang XR, Ma ZX, et al. Multi-objective particle swarm optimization algorithm based on multi-strategy improvement for hybrid energy storage optimization configuration. *Renew Energy* 2024;223:120086.
- [33] Chaudhari P, Thakur AK, Kumar R, Banerjee N, Kumar A. Comparison of NSGA-III with NSGA-II for multi objective optimization of adiabatic styrene reactor. *Mater Today Proc* 2022;57:1509–14.
- [34] Geng Z, Wang Z, Zhu Q, Han Y. Multi-objective operation optimization of ethylene cracking furnace based on AMOPSO algorithm. *Chem Eng Sci* 2016;153:21–33.
- [35] Agrawal N, Rangaiah GP, Ray AK, Gupta SK. Multi-objective optimization of the operation of an industrial low-density polyethylene tubular reactor using genetic algorithm and its jumping gene adaptations. *Ind Eng Chem Res* 2006;45(9):3182–99.
- [36] Nabavi SR, Rangaiah GP, Niaei A, Salari D. Multiobjective optimization of an industrial LPG thermal cracker using a first principles model. *Ind Eng Chem Res* 2009;48(21):9523–33.
- [37] Berreni M, Wang M. Modelling and dynamic optimisation for optimal operation of industrial tubular reactor for propane cracking. *Comput Aided Chem Eng* 2011;29:955–9.
- [38] Shen F, Wang M, Huang L, Qian F. Exergy analysis and multi-objective optimisation for energy system: a case study of a separation process in ethylene manufacturing. *J Ind Eng Chem* 2021;93:394–406.